IEEE Access
Multidisciplinary | Rapid Review | Open Access Journal

Received July 6, 2019, accepted July 29, 2019, date of publication August 6, 2019, date of current version August 28, 2019.

Digital Object Identifier 10.1109/ACCESS.2019.2933573

Cross Layer Optimization of Wireless Control Links in the Software-Defined LEO Satellite Network

WONCHEOL CHO, (Student Member, IEEE), AND JIHWAN P. CHOI, (Senior Member, IEEE)
Department of Information and Communication Engineering, Daegu Gyeongbuk Institute of Science and Technology (DGIST), Daegu 42998, South Korea

Corresponding author: Jihwan P. Choi (jhchoi@dgist.ac.kr)

This work was supported in part by the Institute of Information and communications Technology Planning and Evaluation (IITP) Grant from the Ministry of Science and ICT (Key Technologies Development for Next-Generation Satellites) under Grant 2018-0-01658, and in part by the DGIST Research and Development Program of the Ministry of Science and ICT under Grant 18-ST-02.

ABSTRACT The low earth orbit (LEO) satellite network can benefit from software-defined networking (SDN) by lightening forwarding devices and improving service diversity. In order to apply SDN into the network, however, reliable SDN control links should be associated from satellite gateways to satellites, with the wireless and mobile properties of the network taken into account. Since these characteristics affect both control link association and gateway power allocation, we define a new cross layer SDN control link problem. To the best of our knowledge, this is the first attempt to explore the cross layer control link problem for the software-defined satellite network. A logically centralized SDN control framework constrained by maximum total power is introduced to enhance gateway power efficiency for control link setup. Based on the power control analysis of the problem, a power-efficient control link algorithm is developed, which establishes low latency control links with reduced power consumption. Along with the sensitivity analysis of the proposed control link algorithm, numerical results demonstrate low latency and high reliability of control links established by the algorithm, ultimately suggesting the feasibility, both technical and economical, of the software-defined LEO satellite network.

INDEX TERMS Software-defined satellite network, control link, cross-layer optimization, power-efficient control link algorithm.

I. INTRODUCTION

Satellite networks have an advantage of global coverage and play a role as wireless backhaul for terrestrial communication networks even when the ground infrastructure is destroyed due to disasters. Despite these distinct strengths the main applications of satellite networks have been restricted to telephony or TV broadcasting. Network functionalities have been generally placed on ground hubs where most decisions on data routing are conducted on behalf of satellites, which makes it difficult to provision diverse services. However, the extension of satellite service diversity over the last few decades is now heading to the provisioning of global Internet services through low earth orbit (LEO) satellite networks. Furthermore, the cost-competitive CubeSat network has been recently researched as a platform of the large-scale Internet of Things (IoT) [1]. As the satellite services rapidly catch up with terrestrial counterparts, network functionalities over satellite networks have been actively researched [2]–[4]. Main streams of research work can be divided into two promising concepts: Onboard processing (OBP) satellites which decide data forwarding and packet routing on the payload, and software-defined networking (SDN) which manages the control plane of the satellite network in the software-defined manner.

Owing to the advancement of application-specific integrated circuits (ASIC) and central processing units (CPU), OBP satellites are expected to conduct routing and scheduling decisions on the sky [2]. OBP satellites avoid unnecessary round-trip delays between satellites and ground hubs, thus reducing latency for control message establishment. They, however, require high computation power on the payload, which results in an increase in weight and complexity. Although these burdens are not a big problem for

The associate editor coordinating the review of this manuscript and approving it for publication was Taufik Abrao.

geosynchronous earth orbit (GEO) satellites, they can be a critical influence on survival of LEO satellites, especially for CubeSats [5]. In order to simultaneously meet the payload limitation of the LEO satellite and provide the network functionality on the satellite, SDN is one of the appropriate candidates for the LEO satellite, with simple and light forwarding devices enabled by SDN [6].

Through the placement of virtual network functions (VNFs) such as deep packet inspection (DPI) or load balancing [7], the software-defined satellite network, previously introduced in [4], [8], can provide services which require diverse quality-of-service (QoS). The LEO satellite network with a short propagation delay less than 10 ms is expected to support these diverse QoS requirements. Unlike the traditional network, the propagation delay between the controller and forwarding devices also affects the latency for establishment of the packet handling rules in SDN [9]. Especially in case of event handling reactive to emergency situations such as traffic congestion or link cessation, large latency is fatal to the network performance. Prior to the packet forwarding or event handling, the round-trip propagation delay of GEO satellites, as high as 250 ms, is not suitable for the software-defined satellite network which is anticipated as the platform of diverse services. Instead, as the characteristics of GEO and LEO satellites are taken into account, GEO satellites are expected to be backhauls for the software-defined LEO satellite network for satellite application services.

Traditional communication networks implement both control and data planes in the same purpose-built network devices, which results in inflexibility and high CAPEX/OPEX for upcoming data demand for the 5G applications [6], [10], [11]. SDN has been promised as an approach to overcome the problems of existing ossified networks. Its main features compared to those of conventional networks are as follows [6], [12], [13]: The control plane is logically centralized while the data plane is physically distributed. The SDN controller provides packet handling rules to forwarding devices based on the abstract network view through the open southbound application programming interface (API). The abstract network view enables the management plane to simply manage network reconfigurations or to facilitate introduction of new abstraction.

An architecture for the software-defined LEO satellite network is delineated in Fig. 1. Software-defined satellites serve user equipment through 5G new radio (NR) gNodeBs (gNBs), home-equipped gateways, or directly. A hub consists of a satellite gateway, a network control center (NCC), a network management center (NMC), and a performance-enhancing proxy (PEP). NCC and NMC manage the terrestrial-satellite network through control plane functions and management plane functions respectively [14]. PEP improves end-to-end performances of the whole network by splitting ground wired links and lossy gateway-satellite links (GSLs) at the Transport layer. Satellites and switches on the backbone network are software-defined, and routing/scheduling decisions are conducted on the ground SDN

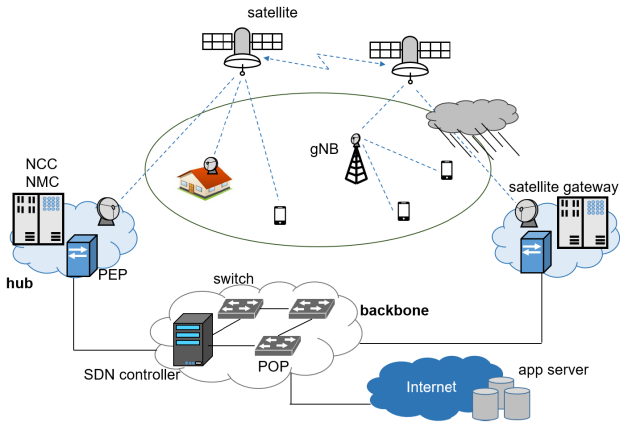

FIGURE 1. An architecture for the software-defined LEO satellite network.

controller located in the backbone network. Along with the decision functionality, the SDN controller establishes control links from the controller to all the satellites. However, weather attenuation at high frequencies beyond Ku and Ka bands can be severe. To adopt SDN to the satellite environment, accordingly, reliable control links should be associated from the SDN controller to all the satellites, taking the extreme wireless characteristics of the LEO network into account.

Average latency minimization of control link setup is the foremost objective of the SDN controller [3], [9]. The control messages with rules of forwarding and routing should be transmitted to each node before data packets arrive at the node. Therefore, the control link latency can have a critical influence on the latency of data transmission, which is directly related to QoS. Given that a control message generally has a small packet size and is prioritized over data, time-varying propagation delay and control link reliability dominantly impinge on the link latency. Link reliability can be represented as an outage probability dependent on the gateway power, explained further in Section III. The gateway power is generally high in the software-defined satellite network owing to the frequent update of control messages and extreme weather attenuation and fading. Further discussion will be held in Subsection III-C. Although maximum power allocation can achieve full reliability, power efficiency of gateways has become increasingly important for the sake of network greenness [15]–[17]. In addition, gateways are generally located at power-limited remote areas where power control is of great importance. The gateway power allocation and the control link association are closely related with the channel environment, which should be optimized in a coupled manner. We define this coupled problem as an SDN control link problem and tackle it with a cross layer approach, for realization of the software-defined LEO satellite network. The main contribution points of this paper are as follows:

- To the best of our knowledge, this paper is the first to deal with the cross layer control link problem in the

software-defined satellite network. The problem minimizes the expected latency that is a function of propagation delay and gateway power. To fully comprehend the software-defined satellite network, a logically centralized control framework constrained by the maximum total power P_{ctrl} is elaborated, which is introduced for the purpose of gateway power efficiency.

- Since the control link problem is prohibitive in computational complexity due to combinatorial link association, a sub-optimal link algorithm with polynomial complexity is proposed. Based on the solid analysis of the SDN control link problem, we propose a power-efficient control link algorithm which establishes low latency control links while reducing power consumption of link setup.
- A large volume of research work has addressed data routing problems in the software-defined wireless network, whereas the feasibility of applying SDN into the satellite network has not been investigated thoroughly. Through the numerical results of the proposed control link algorithm, we analyze the feasibility from the perspective of latency and reliability. This approach additionally lays a cornerstone for a general wireless SDN control link problem of applying SDN into a network of flying objects, such as satellites, unmanned aerial vehicles (UAVs) and high altitude platforms (HAPs).
- It will be shown that latency and reliability of control links established by the proposed control link algorithm are directly affected by the maximum total power P_{ctrl}. To fully exploit the power efficiency of the proposed algorithm, we analyze the local sensitivity and stability of the algorithm with respect to P_{ctrl}. Perturbation analysis and latency observation present an appropriate value of P_{ctrl} above a point of diminishing returns, which simultaneously provides low latency and high reliability.

The rest of this paper is organized as follows: Section II introduces the related work which have proposed the control framework of satellite networks and attempted to apply SDN to satellites as a recent move. In Section III, the scenario of the software-defined LEO satellite network is elaborated, followed by the SDN control link problem formulation. Based on the analysis of the power-efficient control link problem in Section III, we propose a power-efficient control link algorithm in Section IV. The latency performance and stability of the algorithm are analyzed in Section V, which proposes the feasibility of applying SDN to the LEO satellite network. Section VI concludes the paper and presents future work.

II. RELATED WORK

Traditionally, as the LEO satellite network has functioned as a backbone, there have been several studies to adopt connection-oriented asynchronous transfer mode (ATM) or multi-protocol label switching (MPLS) protocols, which are widely exploited in a core cloud of the terrestrial network, into the LEO satellite network [18], [19]. Especially, in [19], a control framework of the MPLS-based satellite network is proposed and the importance of a centralized control station is emphasized. The author in [20] demonstrated the network routing concept in the ATM-based satellite network with inter-satellite links (ISLs).

In recent years, there have been many research outcomes attempting to adapt the control framework of the satellite network to SDN. The authors in [4] applied various concepts such as VNF, software-defined radio (SDR) and SDN to the satellite network, and constructed a scenario of the software-defined satellite network. Its advantages such as integration of terrestrial and satellite networks are introduced in [21]. In [14], the reliability of the satellite backhaul is introduced as along with the advantages of SDN. However, the wireless control link is not explained in detail and the paper lacks the consideration on viability of implementing SDN on the satellite. The authors in [22] proposed a control framework where the physically distributed controllers are mounted on LEO satellites, called control satellites. While ISLs guarantee reliable connections between control and data satellites, the extra cost of link state synchronization between control satellites are required in comparison with fixed ground SDN controllers. Meanwhile, other research work has focused on the network performance analysis of adopting SDN to the LEO satellite network [23]–[25]. A couple of papers proposed congestion avoidance or traffic engineering algorithms based on SDN and achieved better performance over the existing LEO satellite network [23], [24]. The authors in [25] demonstrated throughput improvement for the steady state and the handover state by exploiting SDN.

We demonstrate the feasibility of the software-defined satellite network by proposing a wireless SDN control link algorithm. Unlike our approach here, most of previous studies have addressed the controller placement problem to resolve how to apply SDN to large scale networks [9], [26], [27]. In [9], the SDN controller placement problem was first proposed, which presented the feasibility of adopting SDN into the large scale network. In the satellite network, on the other hand, dynamic control satellite placement in the LEO satellite network was addressed in [28], and the joint placement of controllers and satellite gateways in the software-defined satellite-terrestrial network was solved in [3]. These papers, however, did not take wireless channels and power allocation into account.

III. MODELING AND FORMULATION

A. GRAPH MODEL AND CONTROL LINK ASSOCIATION

The topology of the software-defined satellite network is depicted in Fig. 2. For the control plane, ground SDN controllers manage a set of satellite gateways $\mathbf{W} = \{g_1, g_2, \cdots, g_M\}$ and software-defined LEO satellites $\mathbf{S} = \{s_1, s_2, \cdots, s_N\}$, where M and N are the number of gateways and satellites, respectively. Controllers gather channel state information (CSI) of the network and compose the abstract network view. There are more satellites around the world than

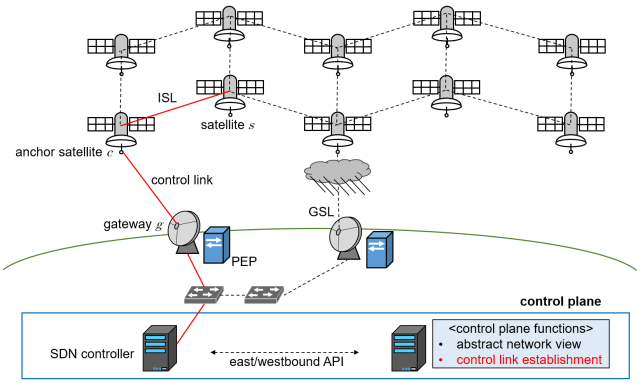

FIGURE 2. Topology of the software-defined LEO satellite network and control link establishment.

gateways in general ($M < N$). Controllers are physically distributed all over the world to cover the global satellite network. In order to retain the logically centralized control plane, controllers share network knowledge through the open east/westbound API [6].

An example control link is associated between a controller and satellite s through gateway g as a red solid line in Fig. 2. In the example, the controller associates the link with the shortest path, while avoiding unreliable channels suffering from weather attenuation. Since M is smaller than N and gateways are not always inside the footprint of each satellite, several satellites should receive control messages from the same satellites through ISL. These satellites play a role of the anchor points in the network [29], and we call them anchor satellites (denoted as c in Fig. 2). The control link has possibly multiple hops through the controller, the gateway, the anchor satellite, and ISL if necessary.

The GSL, whose lossy channel characteristics impinge on transmit control protocol (TCP) connection, is separated from the ground wired link at the Transport layer by the PEP located at the hub. We represent the terrestrial-satellite network as a graph $G(V, E)$, with vertices $V = \mathbf{S} \cup \mathbf{W}$ and edges E which consists of GSLs and ISLs, except for ground wired links. Note that the control link should be established from the controller to each satellite $s \in \mathbf{S}$, over which control messages toward satellite s are transmitted. We introduce an indicator variable $x_{ij}^{(s)} \in \{0, 1\}$ which is 1 when edge $\{i, j\} \in E$ is a part of the control link for satellite s. If satellite s is a destination of a control message, it can be described with the indicator variables as

$$\sum_{i:\{i,s\}\in E} x_{is}^{(s)} - \sum_{i':\{s,i'\}\in E} x_{si'}^{(s)} = 1. \tag{1}$$

SDN employs connection-oriented TCP establishment [30]. For a reliable connection of the control link, especially a connection via GSL, the automatic repeat request (ARQ) protocol controls errors based on retransmissions. The transmitter (gateway) retransmits a control message to the receiver (satellite) if the gateway receives a negative acknowledgement (NACK) or does not receive any feedback within an elapsed time (round-trip propagation delay in this paper without loss of generality). As the transmitter waits for a round-trip propagation delay, a control message setup time under condition of no retransmission equals the round-trip propagation delay of the control link. Here transmission and queueing delays are negligible compared to propagation delays, since a control message generally has a small packet size and is prioritized over data. Given a control message toward satellite s that satisfies Eq. (1) and gateway $g \in \mathbf{W}$ from which the control message originates, the control message setup time d_{gs} from g to s can be formulated as follows:

$$d_{gs} = \sum_{\{i,j\}\in E} x_{ij}^{(s)} d_{ij}, \tag{2}$$

where d_{ij} is a round-trip propagation delay of edge $\{i, j\}$. Note that the selection of gateway g is dependent on the indicator variable $x_{ij}^{(s)}$, which can be represented as $\sum_{i:\{g,i\}\in E} x_{gi}^{(s)} = 1$.

Each satellite gateway has a tracking antenna, enabling a GSL between the anchor satellite and the gateway for a time slot, which is described as

$$\sum_{g\in\mathbf{W}} \sum_{i:\{g,i\}\in E} x_{gi}^{(s)} = 1. \tag{3}$$

Additionally, given gateway set $\mathbf{W}$ and satellite s, data flow between intermediate vertices should be conserved under the constraint given as

$$\sum_{j:\{i,j\}\in E} x_{ij}^{(s)} - \sum_{j':\{j',i\}\in E} x_{j'i}^{(s)} = 0, \quad \forall i \notin \{s\} \cup \mathbf{W}. \tag{4}$$

B. CONTROL LINK RELIABILITY AND EXPECTED LATENCY FORMULATION

Control link reliability can be represented as an outage probability. When control links are established, link outages should be avoided because they incur retransmissions with redundant power consumption and increased latency. We suppose that the controllers, managing the global-scale network topology, have large-scale channel knowledge of ISL and GSL, which mainly consists of weather attenuation and path loss. Under the condition of line-of-sight (LOS) between gateways and satellites, GSL is modeled to follow small-scale Nakagami fading [31], and only the knowledge of channel distribution is available to the controllers. The shape factor $m = 1$ implies that the channel suffers Rayleigh fading and m gradually increases as the strength of the specular scattered signal increases compared to diffuse scattering. ISL is only affected by the propagation distance, owing to a good channel condition at the altitude above 200 km. The connection causing the control link outage toward s is the GSL between gateway g such that $\sum_{i:\{g,i\}\in E} x_{gi}^{(s)} = 1$ and anchor satellite c such that $x_{gc}^{(s)} = 1$. Anchor satellite c sometimes is identical to satellite s, depending on the topology of the satellite network. The link outage probability between g and c has the closed form as below [32]:

$$P_{gc}^{\text{out}} = 1 - \frac{\Gamma\left(m, \frac{m\gamma_{th}}{\gamma_{gc}}\right)}{\Gamma(m)}, \tag{5}$$

where γ_{th} is the signal-to-noise ratio (SNR) threshold required for receiving a control message, and $\bar{\gamma_{gc}}$ is the average received SNR at anchor satellite c. $\Gamma(m)$ is the gamma function and $\Gamma(m, m\gamma_{th}/\bar{\gamma_{gc}})$ is the upper incomplete gamma function [33, Eq.(6.5.3)]. The average SNR $\bar{\gamma_{gc}}$ is written as

$$\bar{\gamma_{gc}} = \frac{H_{gc}P_g}{WN_0}, \tag{6}$$

where H_{gc} and P_g are the large-scale channel gain and the transmit power from gateway g to anchor satellite c, respectively, W is the uplink bandwidth, and N_0 is the noise power density. Large-scale channel gain $H_{gc} = \alpha_g \cdot l_{gc}$ consists of free space path loss l_{gc} and weather attenuation α_g. Path loss l_{gc} is modelled as $l_{gc} = \left(\frac{\sqrt{G_{gc}}f}{2\pi d_{gc}}\right)^2$ [34], where G_{gc} is the product of antenna field radiation patterns of gateway g and anchor satellite c, f is the carrier frequency, and d_{gc} is the round-trip propagation delay between gateway g and anchor satellite c.

We define the number of transmissions N_{gc} for control message setup from gateway g to anchor satellite c caused by outages under the condition of $P_g > 0$ ($N_{gc} = 0$ for $P_g = 0$). Since LEO satellites move at high speeds along orbits (e.g., 7.16 km/s at altitude 1,400 km), channels between gateways and satellites suffer from fast small-scale fading and each transmission trial is assumed to be an independent and identically distributed (i.i.d.) Bernoulli random variable with success probability $1 - P_{gc}^{\text{out}}$. Thus, the number of transmissions N_{gc} follows geometric distribution [35], whose ensemble average $\mathbb{E}[N_{gc}]$ is given as

$$\mathbb{E}[N_{gc}] = \frac{1}{1 - P_{gc}^{\text{out}}} = \frac{\Gamma(m)}{\Gamma\left(m, \frac{m\gamma_{th}}{\bar{\gamma_{gc}}}\right)}. \tag{7}$$

With control message setup delay d_{gs} represented as Eq. (2) and the average number of transmissions as Eq. (7), the expected steady-state latency L_{gs} of control message establishment from g to s is expressed as

$$L_{gs} = \sum_{\{i,j\}\in E} x_{ij}^{(s)} d_{ij} \mathbb{E}[N_{gc}], \tag{8}$$

which is a function of indicator variables $x_{ij}^{(s)}$ and gateway transmit power P_g. The expected latency L_{gs} is convex with respect to transmit power P_g, under the condition that the shape factor m is an integer with the proof given in Appendix A. Fig. 3 presents the expected latency as a function of transmit power by changing the shape factor and weather attenuation. Under mild weather conditions, as expected, gateways located at the LOS environment without obstruction (i.e., large m) serve lower expected latency L_{gs}, and L_{gs} is reduced by transmitting large power P_g. Under harsh weather attenuation, on the other hand, the lowest expected latency of Rayleigh fading ($m = 1$) is achievable in the low transmit power region, since well-scattered signals can prevent outages. As the shape factor m increases,

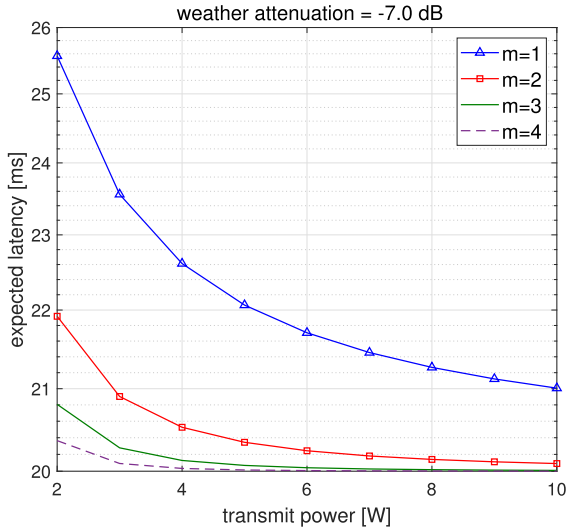

(a) Expected latency under mild weather conditions

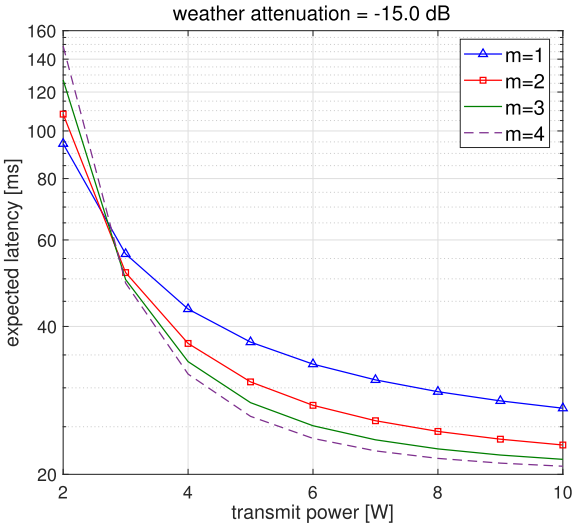

(b) Expected latency under harsh weather conditions

FIGURE 3. Expected latencies by changing transmit power under the condition of different weather attenuation and round-trip propagation delay 20 ms, including ISL transmissions.

additional power consumption greatly reduces the expected latency. Since satellite gateways are usually located where the shape factor is high (i.e., free from obstructions), large marginal returns of the expected latency in the low power region are a crucial factor to efficiently reduce gateway power consumption.

Given a feasible control link association variable $x_{ij}^{(s)}$, the derivative $\frac{\partial L_{gs}}{\partial P_g}$ with respect to gateway transmit power $P_g > 0$ is always negative and formulated as

$$\frac{\partial L_{gs}}{\partial P_g} = -\frac{d_{gs}H_{gc}}{WN_0} \cdot \frac{\Gamma(m)}{\bar{\gamma_{gc}}} \cdot \left\{\frac{1}{\Gamma(m, \frac{m\gamma_{th}}{\bar{\gamma_{gc}}})}\right\}^2 \times \left(\frac{m\gamma_{th}}{\bar{\gamma_{gc}}}\right)^m \cdot e^{-\frac{m\gamma_{th}}{\bar{\gamma_{gc}}}}, \tag{9}$$

which implies that the expected latency monotonically decreases with respect to P_g. Hence a cross layer approach (P_g and $x_{ij}^{(s)}$ as optimization variables) to minimize the expected latency for each satellite s is reduced into the link association problem with full power allocation. This result shows that gateways are allocated with a sufficient power margin to reduce latency and ensure reliability.

C. POWER-EFFICIENT SDN CONTROL LINK PROBLEM

Regardless of the constellation that the LEO satellite network is designed with, the links between satellites and ground gateways or user equipment always change over time. Even the data with a same origin and a destination can be transmitted by different satellites if the service time differs. Hence, flow tables should be updated according to the time-varying network. Furthermore, as dynamic network slicing, which can be highly facilitated by SDN [36], [37], is implemented in the near future, control updates will increase drastically. Given that the link connection between gateways and LEO satellites is about 10 minutes, it is necessary to frequently transmit and update control information. In addition, Section V will show that a large amount of power is required to ensure high reliability since the reliability of the control link is largely affected by weather attenuation and fading of the satellite channel. Accordingly, the amount of power consumed for control link setup is generally large. Although the sufficient power margin maximizes reliability, allocating full power leads to power inefficiency incompatible with the perspective of green communication. Furthermore, since gateways are located at power-limited remote areas in general, power efficiency at gateways is one of the most significant factors to realize the software-defined satellite network.

In order to maintain low latency control links while saving power, the controller should exploit the diminishing marginal return of expected latency with respect to power in a cross-layer approach. In Fig. 3, we demonstrate high marginal returns of the expected latency in the low transmit power region under the harsh weather condition, in particular with the large shape factor m. For instance, the expected latency L_{gs} decreases to about 17 ms if P_g increases from 3 to 4 W, while it decreases to less than 1 ms if P_g increases from 7 to 8 W with $m = 4$. A logically centralized SDN control framework is exploited to moderate power consumption for control link setup by introducing the maximum total power, and we formulate the power-efficient SDN control link problem given as

$$\min_{P_g, x_{ij}^{(s)}} \quad \frac{1}{N} \sum_{g \in \mathbf{W}} \sum_{s \in \mathbf{S}} L_{gs} \tag{10}$$

$$\text{s.t.} \quad P_g \le P_{GW}, \quad \forall g \in \mathbf{W}, \tag{11}$$

$$\sum_{g \in \mathbf{W}} P_g \le P_{ctrl}, \tag{12}$$

$$(1), (3), (4), \quad \forall s \in \mathbf{S},$$

where P_{GW} is the maximum power amount available for the gateway and P_{ctrl} is the maximum total power required for control link setup, which directly affects both power consumption and latencies of SDN control links. The maximum total power P_{ctrl} is established by the management plane. In general, the per-node average latency, same as Eq. (10), is set as an objective function in the controller placement problem [3], [26], which minimizes the average latency by searching the optimal placement of controllers. On the other hand, the proposed SDN control link problem seeks the optimal link association $x_{ij}^{(s)*}$ and power allocation P_g^* jointly.

The power-efficient control link problem holds strong duality with respect to power P_g with Slater's condition satisfied [38]. Then the optimal solution derived by the Karush-Kuhn-Tucker (KKT) condition is also the primal optimal. Given feasible control link association variable $x_{ij}^{(s)}$, the optimally allocated power of each gateway g is obtained by solving the equation given as

$$\frac{1}{N} \left. \frac{\partial L_{gs}}{\partial P_g} \right|_{P_g = P_g^*} + \lambda_g = -\Lambda < 0, \tag{13}$$

where λ_g and Λ are Lagrangian multipliers associated with the gateway power constraint in Eq. (11) and the maximum amount of the total power in Eq. (12), respectively. Gateway power allocation can be divided into two cases: 1) $P_g^* = P_{GW}$ ($\lambda_g \ge 0$), where the transmit power of gateway g is at the maximum value, or 2) $P_k^* < P_{GW}$ ($\lambda_k = 0$), where the transmit power of gateway k is not saturated. Then the following inequality holds:

$$\left. \frac{\partial L_{gs}}{\partial P_g} \right|_{P_g = P_g^*} \le \left. \frac{\partial L_{ks}}{\partial P_k} \right|_{P_k = P_k^*} = -N\Lambda, \tag{14}$$

where $P_k^* < P_g^* = P_{GW}$. Due to the convexity of the expected latency L_{gs} with respect to transmit power, the derivative in Eq. (14) becomes larger as the amount of power increases under the condition of fixed weather attenuation and round-trip propagation delay. However, owing to the different weather conditions of gateways and various propagation delay for each satellite, the inequality in (14) holds for power allocation $P_k^* < P_g^*$. The impact of weather attenuation α_g and round-trip propagation delay d_{gs} on the derivative of the expected latency is depicted in Fig. 4, with gateway power P_g fixed at a certain amount P_0 (e.g., 5 W in Fig. 4). The z-axis represents the derivative with respect to the allocated power, $\left. \frac{\partial L_{gs}}{\partial P_g} \right|_{P_g = P_0}$. As the gateway suffers from much severe weather attenuation or longer round-trip propagation delay between g and s, $\left. \frac{\partial L_{gs}}{\partial P_g} \right|_{P_g = P_g^*}$ decreases. Then Eq. (14) denotes that, given an associated control link represented with $x_{ij}^{(s)}$, a large amount of power should be allocated to the satellite in severe weather attenuation or at a long distance. The satellites served by gateways under severe weather attenuation are allocated more power because they are prone to outages. Repetitive outages result in control performance degradation in the whole network. The satellites at a longer distance are also allocated more power since the latency caused by retransmissions is

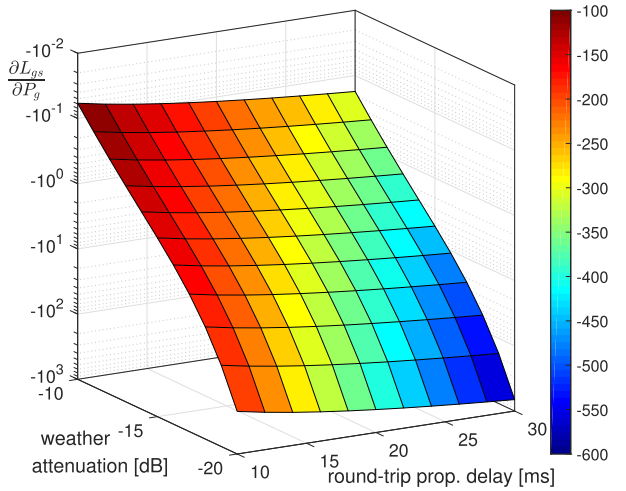

FIGURE 4. The derivative $\frac{\partial L_{gs}}{\partial P_g}\Big|_{P_g=P_0}$ by changing weather attenuation and round-trip propagation delay.

much larger than the satellites at a shorter distance. Especially, the derivative decreases rapidly as weather attenuation becomes severe, indicating that weather attenuation increases power consumption more than the long propagation delay.

The result can be interpreted from a viewpoint of link association which is coupled with the power allocation problem. Through the power control analysis, given the link association, much power is allocated to the satellite with lower $\frac{\partial L_{gs}}{\partial P_g}\Big|_{P_g=P_0}$. On the other hand, under the fixed power allocation, links with larger $\frac{\partial L_{gs}}{\partial P_g}\Big|_{P_g=P_0}$ should be associated to reduce power consumption since a large value of the derivative is the necessary and sufficient condition for saving power allocation. Hence, in order to minimize the average control link latency while reducing power allocation, the optimally associated link is with large $\frac{\partial L_{gs}}{\partial P_g}\Big|_{P_g=P_0}$ by avoiding association with a gateway suffering from a severe weather condition and/or to a distant satellite as indicated in Fig. 4.

IV. SDN CONTROL LINK ALGORITHM

The controller requires the knowledge of round-trip propagation delay and weather attenuation of the whole network in order to calculate the average number of transmission $\mathbb{E}[N_{gc}]$ caused by outages. The path loss is predictable because the satellite constellation operates in a pre-determined way, and the knowledge of quasi-static weather attenuation, whose coherence time is longer than the control link latency in general, can be achieved by frequently probing channel states. Hence, periodic probing of weather conditions and path loss is sufficient for the controllers to be aware of d_{ij} and H_{gc}. For coherent network knowledge of SDN controllers, periodic synchronization is performed through open west/eastbound API. In addition, to respond rapidly to an event that causes network congestion or link cessation, satellites report the network problems to the control plane in real-time.

Based on the abstract network view, the control plane operates control link algorithms in both proactive (periodic) and reactive (event-triggered) manners. In the steady state, it is sufficient for SDN controllers to establish control links periodically. However, unpredictable link congestion and outages require new traffic engineering in real-time. Thus, the control link algorithm should establish low latency control links with low computational complexity to tackle events rapidly.

The power-efficient SDN control link problem searches all the feasible links to simultaneously solve link association and power allocation. A brute-force recursive algorithm to find all the feasible links between gateway g and satellite s has complexity in the order of $\mathcal{O}(N!)$, which makes the control plane difficult to operate in an event-triggered manner. We propose a sub-optimal algorithm that has polynomial complexity but guarantees low latency on this account. A key idea of the algorithm is that $\frac{\partial L_{gs}}{\partial P_g}\Big|_{P_g=P_0}$ acts as a hinge [2], [39], decoupling link association and power allocation. From the analysis of the power-efficient SDN control link problem in Section III, the link with the largest $\frac{\partial L_{gs}}{\partial P_g}\Big|_{P_g=P_0}$ is selected as an optimal control link for each s. As demonstrated in Fig. 4, weather attenuation has a worse impact on the derivative than propagation delay. Note that a link associated with enough power is mainly affected by propagation delay with the small outage probability, while a link with small gateway power is heavily affected by weather attenuation. Based on these observations, for every satellite $s \in \mathbf{S}$, the controller establishes a control link with small power P_{small} which is expected to have a large value of $\frac{\partial L_{gs}}{\partial P_g}\Big|_{P_g=P_0}$. Following the link association represented by $x_{ij}^{(s)}$ for every s, the power-efficient control link problem is reduced into the power allocation problem given as

$$\min_{P_g} \quad \frac{1}{N}\sum_{g\in\mathbf{W}}\sum_{s\in\mathbf{S}} L_{gs} \qquad (15)$$
$$\text{s.t.} \quad (11), (12).$$

The proposed sub-optimal SDN control link algorithm is described in **Algorithm 1**. The link association procedure exploits the shortest path algorithm Shortest_Path() where the input is the round-trip propagation delay weighted by the average number of transmissions, for every $g \in \mathbf{W}$ and every $s \in \mathbf{S}$ to establish control link $x_{ij}^{(g\to s)}$ from g to s. Given that the computation complexity of the simple Dijkstra algorithm is $\mathcal{O}(N^2)$ as the shortest path algorithm, the total complexity of the link association procedure is $\mathcal{O}(MN^3)$, where M is the number of gateways and N is that of satellites, respectively. The power allocation procedure employs the barrier method, which optimizes the inequality-constrained convex problem, to solve the reduced power allocation problem. For example, if we can approximate the expected latency L_{gs} with respect to power P_g as a quadratic function, as seen in Fig. 3a, the third derivative of the objective function (15) can be upper-bounded by the constant value. This makes

Algorithm 1 Power-Efficient SDN Control Link Algorithm

Data: H_{gc}, d_{ij}
Result: P_g, $x_{ij}^{(s)}$
begin
  Initialize P_{small}.
  for *all* $s \in \mathbf{S}$ **do**
    for *all* $g \in \mathbf{W}$ **do**
      $P_g := P_{small}$.
      $\mathbb{E}[N_{gc}] := \Gamma(m)/\Gamma\left(m, \frac{m\gamma_{th}WN_0}{H_{gc}P_g}\right)$.
      $c_{ij} := d_{ij}\mathbb{E}[N_{gc}]$.
      $x_{ij}^{(g\to s)} :=$ Shortest_Path(c_{ij}).
    end
    $x_{ij}^{(s)} := \min_{g\in\mathbf{W}} x_{ij}^{(g\to s)}$.
  end
  Initialize P_g, $\mu > 1$, tolerance ϵ, and parameter $t^{(0)}$.
  $t := t^{(0)}$.
  while $(M+1)/t > \epsilon$ **do**
    $P_g^*(t) := \text{argmin}_{P_g}\left\{\frac{t}{N}\sum_s L_{gs} - \phi\right\}$, $\phi = \sum_g \log(P_{GW} - P_g) + \log(P_{ctrl} - \sum_g P_g)$.
    $P_g := P_g^*(t)$.
    $t := \mu t$.
  end
end

the objective function self-concordant [40], which gives the complexity of the barrier method within the order $\mathcal{O}(\sqrt{M}\log(\frac{M}{t^{(0)}\epsilon}))$, where $t^{(0)}$ is an initial value of the approximation accuracy parameter and ϵ is a tolerance [38]. In summary, the total computation complexity of the proposed control link algorithm is given by

$$\mathcal{O}(MN^3 + \sqrt{M}\log(M)) = \mathcal{O}(MN^3), \tag{16}$$

which is mainly dependent on the link association procedure.

V. NUMERICAL RESULTS AND ANALYSIS

The proposed power-efficient link algorithm is applied to the LEO satellite network for numerical evaluation. We adopt the Walker delta constellation and the detail parameters are referred to as the Celestri constellation [41], [42]. The Walker delta constellation provides permanently maintainable ISLs with acceptable pointing, acquisition, and tracking requirements [19], [43]. However, the time-varying link between the gateway and the anchor satellite, and the resulting handover have a negative impact on the control link reliability. The handover will not be discussed in further detail, and details are referred to [25] which applied multipath TCP connections to solve the handover challenges. On the other hand, the Walker star constellation exploited in Iridium has a seam between counter-rotating planes, and the ISLs between inter-plane orbits change with time [18]. These drawbacks require much effort to obtain the same control link reliability as in the delta constellation.

TABLE 1. Satellite constellation and communication parameters.

Satellite constellation	
No. of satellites	48
No. of planes	8
Orbit inclination	53
Altitude	1,400 km
ISL distance range	5,860 km
Communication parameters	
No. of gateways	27
Uplink distance range	1,800 km
Uplink bandwidth	0.5 GHz
Maximum power	10 W
Shape factor	4
Weather attenuation	-13.01 dB
SNR threshold	-10 dB
Noise power density	4.0×10^{-21} W/Hz

The proposed algorithm can be analyzed in other satellite network constellations with diverse scales of satellites and gateways by the method presented in this section. As the number of satellites increases, the control link latency escalates, and thus more gateways and controllers should be deployed to solve this network scalability problem. The key issues of network scalability are an increment in CAPEX/OPEX due to the increase of gateways and controllers, and the maintenance cost of the coherent control plane through east/westbound API. An analysis for this can be one of further research topics.

Table 1 shows the LEO satellite constellation and communication parameters in the simulation. We set shape factor $m = 4$ because gateways are generally located free from obstructions. Power constraints of all the gateways are assumed to be equal to 10 W without loss of generality. In the simulation, the weather condition follows the two-state Markov process where good and bad weather states are randomly selected every 30 minutes. Under a bad weather condition, the signals transmitted from the gateway are set to have weather attenuation of 13 dB more than under good weather. Satellite gateways are distributed according to the Globalstar gateway locations [44].

Full power link algorithms without/with CSI are compared with the proposed algorithm as benchmarks. Full power algorithm without CSI can be regarded as the control link algorithm employed in the existing software-defined wired network. On the other hand, it is shown in Section III that the expected latency minimization problem reduces to a link association problem with on/off power allocation. Accordingly, the full power link algorithm with CSI is equivalent with the optimal expected latency minimization (ELM) algorithm. The latency comparison with the non-SDN algorithm may be trivial and is not considered here, since SDN has a great advantage of being able to manage the whole network on the centralized control plane.

A. LATENCY ANALYSIS AND FEASIBILITY OF THE SOFTWARE-DEFINED SATELLITE NETWORK

Let δ_s denote the latency for control message establishment of satellite s averaged over 1,000 simulation iterations for

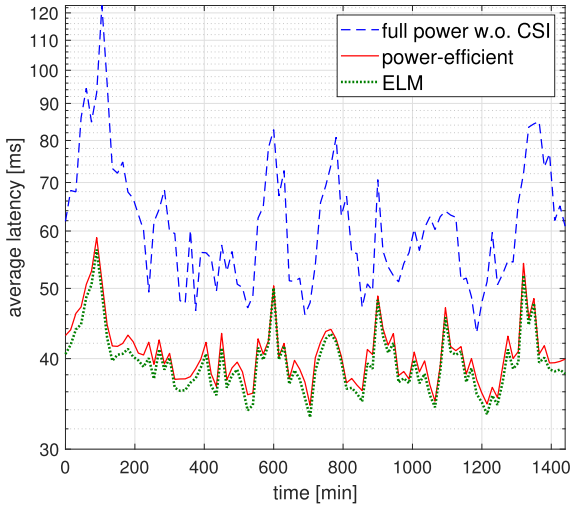

FIGURE 5. Average latency comparison between control link algorithms for 24 hours.

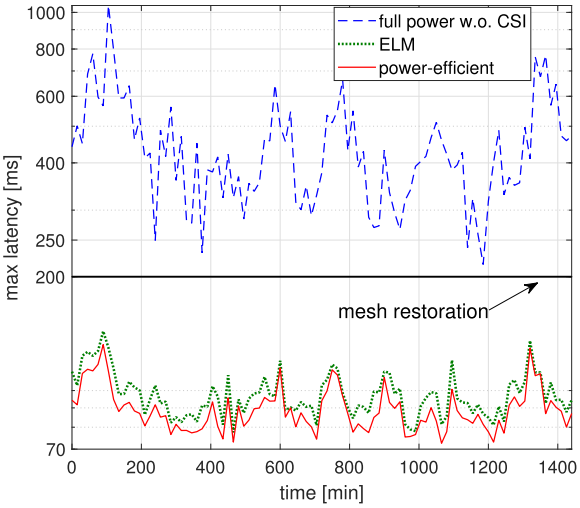

FIGURE 6. Maximum latency comparison between control link algorithms for 24 hours.

TABLE 2. Comparison between control link algorithms.

Algorithm	ELM	Power-efficient
Gateway transmit power per satellite	10.77 W	6.40 W
Running time	13.54 ms	24.69 ms
Asymptotic complexity	$\mathcal{O}(MN^3)$	

the steady-state performance analysis. Retransmission events caused by outages are considered in the measured latency δ_s as a random variable following the outage probability. The metrics of our interest are the average of per-satellite latency $\mathbb{E}[\delta_s]$ and the maximum latency $\max \delta_s$ for every satellite $s \in \mathbf{S}$. Fig. 5 represents the average latency $\mathbb{E}[\delta_s]$ over all the satellites and provides the comprehensive network performance of the proposed algorithm. The maximum total power P_{ctrl} of the power-efficient algorithm is set at 50 W. The daily average of $\mathbb{E}[\delta_s]$ of the power-efficient algorithm is 41.01 ms, while those of ELM and the full power algorithm without CSI are 39.77 ms and 62.35 ms, respectively. The latency performance of the proposed algorithm is comparable with that of the ELM algorithm, only about 3% higher on average.

Table 2 presents the comparison between ELM and the proposed algorithm with respect to gateway transmit power consumption per satellite, running time (both in simulation), and asymptotic complexity. The power-efficient algorithm utilizes the maximum total power $P_{ctrl} = 50$ W. Both gateway transmit power consumption and running time are averaged over 100 simulation iterations. Since the control link problem optimizes power allocation in a time slot in the steady state, real power consumption is taken into account due to the control message transmission based on time division multiple access (TDMA) and/or retransmissions caused by outages. The proposed algorithm, which is the power-constrained version of ELM, markedly reduces the total power consumption for control link setup. Its average value of per-satellite power consumption is only 59% of that of the ELM algorithm. The cross layer approach of the proposed algorithm makes the best use of the diminishing marginal return of the expected latency efficiently, reducing power consumption while preserving average latency performance. Since the ELM algorithm associates the control link by allocating full power P_{GW} to minimize the expected latency, the complexity of the ELM algorithm is $\mathcal{O}(MN^3)$, which is same as the proposed algorithm. Simulation running time, however, shows a significant difference due to the power allocation procedure. While the analytical complexity of the proposed algorithm is mainly dependent on the link association procedure, as derived in Eq. (16), the optimization parameters such as initial point $t^{(0)}$ and tolerance ϵ affect the practical running time in simulations. To sum up, the power-efficient control link algorithm efficiently reduces power consumption of the control framework at the cost of increased running time.

In Fig. 6, the maximum latency $\max \delta_s$ of each algorithm is compared. The maximum total power P_{ctrl} of the power-efficient algorithm is set at 50 W. The maximum latency $\max \delta_s$ indicates the latency of the last satellite in which the control message is established. Since data routing should operate after the establishment of the control message to all satellites, $\max \delta_s$ directly decides QoS requirements and finally becomes the bottleneck of the control link algorithm. Hence, from the perspective of implementation of SDN into the satellite network, the maximum latency can be more critical than the average latency. The maximum latencies of both ELM and the proposed algorithm are extremely lower than that of the control link algorithm without CSI. Interestingly, contrary to the average latency result, the daily average of $\max \delta_s$ of the proposed algorithm is 89.46 ms and that of ELM is 97.90 ms, about 9 % higher.

The results in Fig. 6 also provide the feasibility of operating SDN for LEO satellites. As introduced in Section II, there

have been many prior studies on ATM-based LEO satellite networks [18], [20], which have been deemed as the typical control framework of LEO satellite networks to the date. Accordingly, by comparing the maximum latency $\max \delta_s$ of the algorithms and the mesh restoration time of about 200-250 ms, which is the time duration when ATM circuit rerouting may be triggered [9], [45], it is sufficient to demonstrate the feasibility of applying SDN into the network.[1] The maximum latency $\max \delta_s$ of the full power control link algorithm without CSI always exceeds the mesh restoration time, suggesting that the control link algorithm employed in the wired terrestrial network cannot be applied into the LEO satellite network as it is. On the other hand, the values of $\max \delta_s$ of the ELM and power-efficient algorithm are always much lower than the mesh restoration time. Consuming much less power on the control framework, the proposed algorithm always provides $\max \delta_s$ below the mesh restoration time. The management plane should select P_{ctrl} carefully, considering the trade-off between power consumption and the latency performance, which will be covered in the next subsection.

To comprehend the results accurately, we analyze how each algorithm associates the control links. Fig. 7 represents the averages of per-satellite round-trip propagation delays and outage probabilities of control links established by the three control link algorithms. Results are averaged over 1,000 iterations for the steady-state performance analysis and the maximum total power P_{ctrl} is set at 50 W. First, the full power link algorithm without CSI associates control links with the shortest propagation delay without considering the outage probability. As a result, both the average and the maximum latency grow due to repetitive outages. From the perspective of reliability, the channel-ignorant algorithm (exploited in terrestrial SDN) is not applicable to the wireless network. On the contrary, both the power-efficient and ELM algorithms have the strategy to associate links with the minimum expected latency. The proposed algorithm, however, lacks the absolute power to reduce the outage probability of GSL where the gateway suffers from severe weather attenuation. Accordingly, the proposed algorithm detours to the gateway under a good weather condition, if possible, at the expense of longer propagation delay. On the other hand, the ELM algorithm aggressively exploits the outage probability if the expected latency of the link under severe large-scale fading is lower than that of the detour under mild large-scale fading. Thus, although the per-satellite average latency of ELM is always lower than the power-efficient algorithm,

[1]To strictly prove the feasibility, the network average latency from ground controllers to gateways should be considered together. However, in order to figure out the terrestrial network latency, a comprehensive discussion on the network should be developed, such as the dynamic controller placement problem or the joint controller and gateway placement problem. This is beyond the scope of this paper. Fortunately, the latency analyses on Chinanet [3] and on Internet Topology Zoo [9] confirm that the average latency of China- and US-sized topologies is less than 10 ms. Therefore, if the latency of the satellite network satisfies the mesh restoration time with an enough margin, the latency of the entire network including the global terrestrial network is expected to satisfy the mesh restoration time.

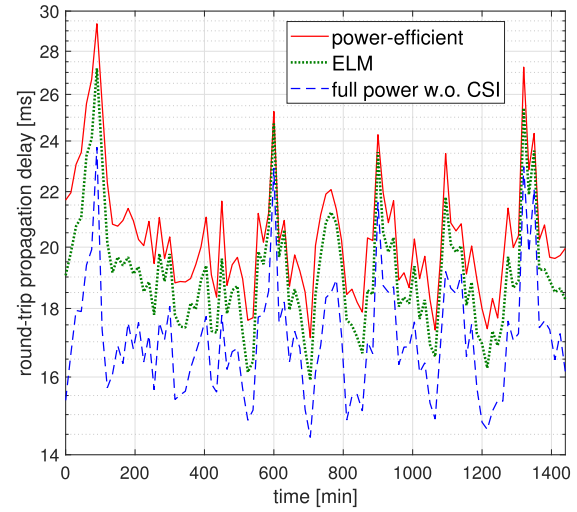

(a) Average round-trip propagation delay

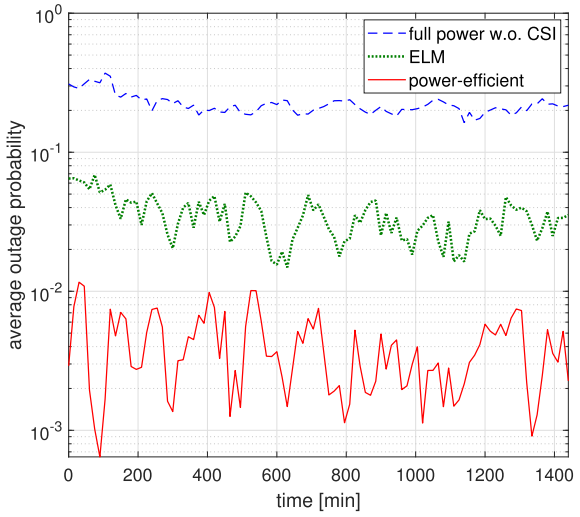

(b) Average outage probability

FIGURE 7. Averages of round-trip propagation delay and per-satellite outage probability of control link algorithms for 24 hours.

the maximum latency of the proposed is lower than that of ELM where the satellite is served by the gateway with a relatively large outage probability.

B. STABILITY OF THE POWER-EFFICIENT CONTROL LINK ALGORITHM AND APPROPRIATE SELECTION OF THE MAXIMUM TOTAL POWER

The maximum total power P_{ctrl} influences both the latency performance and power consumption. Small P_{ctrl} makes gateways consume less power for control link setup but the latency performance can be degraded exponentially. For a proper selection of P_{ctrl}, which is the most critical part of the proposed algorithm, we analyze the sensitivity and stability of the power-efficient control link algorithm through the perturbation [38] and latency analysis. Furthermore, we suggest a valid parameter selection method of P_{ctrl}, which takes advantage of a diminishing law of

the marginal return of sensitivity or stability with respect to P_{ctrl}.

Local sensitivity is the metric to evaluate how sensitive the optimization problem is to the perturbing constraint. For the sensitivity analysis with respect to P_{ctrl}, we formulate a perturbed version of the power-efficient SDN control link problem as below:

$$\min_{P_g, x_{ij}^{(s)}} \quad \frac{1}{N} \sum_{g \in \mathbf{W}} \sum_{s \in \mathbf{S}} L_{gs} \tag{17}$$

$$\text{s.t.} \quad P_g \leq P_{GW}, \quad \forall g \in \mathbf{W}, \tag{18}$$

$$\sum_{g \in \mathbf{W}} P_g - P_{ctrl} \leq u, \tag{19}$$

$$(1), (3), (4), \quad \forall s \in \mathbf{S},$$

where u is a perturbing variable. When $u > 0$ the total power consumption constraint is relaxed; otherwise it is tightened. Let L_{avg}^* and $L_{avg}^*(u)$ be the optimal values of the power-efficient SDN control link problem and the perturbed problem, respectively. Then we have the following inequality which provides the lower bound of $L_{avg}^*(u)$:

$$L_{avg}^*(u) \geq L_{avg}^* - \Lambda u, \tag{20}$$

where Λ is a Lagrangian multiplier associated with the maximum amount of the total power. With perturbation relaxed for $u > 0$, Eq. (20) yields the following as $u \to 0$:

$$\left. \frac{\partial L_{avg}^*(u)}{\partial u} \right|_{u=0} \geq -\Lambda. \tag{21}$$

While the opposite inequality holds for $u < 0$ with tightened perturbation, we can obtain the local sensitivity of the power-efficient control link problem with respect to P_{ctrl}:

$$\left. \frac{\partial L_{avg}^*(u)}{\partial u} \right|_{u=0} = -\Lambda. \tag{22}$$

Fig. 8 demonstrates the local sensitivity $\left. \frac{\partial L_{avg}^*(u)}{\partial u} \right|_{u=0}$ of the perturbed power-efficient SDN control link problem by changing the maximum total power P_{ctrl} from 25 W to 85 W. Monte Carlo simulations take 100 iterations for the steady-state performance analysis and the error bars indicate the maximum and minimum values of local sensitivity which deviate from the mean (i.e., a confidence interval with 100 percent). Small values of local sensitivity indicate that the relaxation of the total power consumption constraint greatly decreases the per-satellite average of the expected latency $L_{avg}^*(u)$. The local sensitivity of the problem increases greatly by increasing P_{ctrl}, with a concave trend. The concavity manifests the point of diminishing returns where the maximum total power efficiently decreases local sensitivity. A gradient in the low P_{ctrl} region is steeper because the satellites served by gateways under bad weather or at a long distance cannot be provided with power enough to

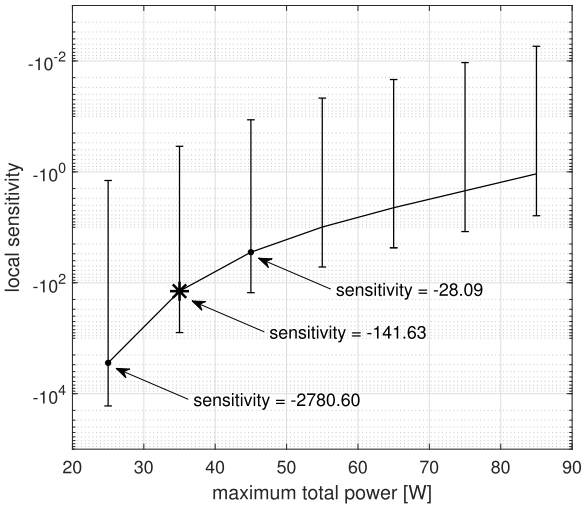

FIGURE 8. Local sensitivity of the power-efficient SDN control link problem by changing maximum total power P_{ctrl}.

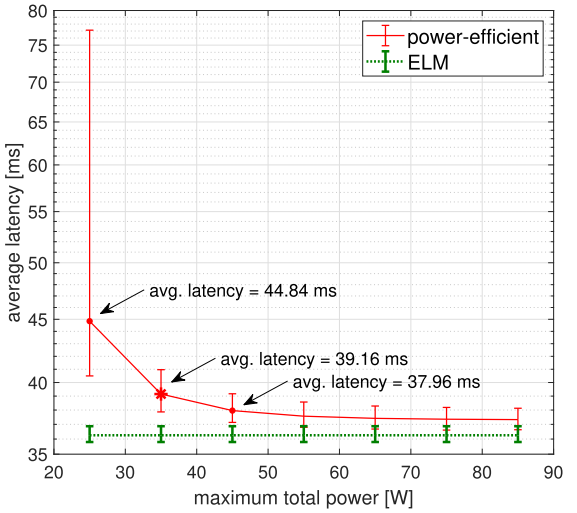

FIGURE 9. Average latency of ELM and power-efficient algorithms by changing maximum total power P_{ctrl}.

reduce the average of the expected latency. Hence by exploiting the diminishing marginal returns of local sensitivity, we indicate P_{ctrl} equal to 35 W as the point of diminishing returns. In detail, local sensitivity dramatically increases from -2780.60 to -141.63 as P_{ctrl} increases from 25 to 35 W. However, local sensitivity increases smaller from -141.63 to -28.09 as P_{ctrl} increases from 35 W to 45 W, above the point of diminishing returns. Thus, from the local sensitivity analysis, a proper value of the maximum total power is suggested at 45-55 W, which is above the point of diminishing returns (35 W).

Fig. 9 shows the convergence of the daily average of $\mathbb{E}[\delta_s]$ of the power-efficient algorithm toward that of the ELM algorithm, by changing the maximum amount of total power P_{ctrl}. Monte Carlo simulations take 100 iterations for the steady-state performance analysis and 100 percent confidence intervals are given as error bars. Since the ELM

algorithm is independent of P_{ctrl}, the average latency is presented as a constant. Although the average latencies of the two algorithms do not make a large difference on the whole P_{ctrl} region, the daily average of $\mathbb{E}[\delta_s]$ of the proposed algorithm converges quickly to that of ELM as P_{ctrl} increases. In addition, the time averages of $\mathbb{E}[\delta_s]$ of the proposed algorithm and ELM are almost the same when P_{ctrl} is larger than 45 W while the control framework with the proposed algorithm uses much less power than that with ELM algorithm, which presents the power efficiency of the proposed algorithm. Interestingly, similar to the sensitivity analysis, the stability analysis also suggests the point of diminishing returns at 35 W. Hence, the management plane should set the maximum total power at 45-55 W above the point.

In addition, as the maximum total power P_{ctrl} becomes smaller, the deviation of local sensitivity in Fig. 8 and that of the daily average of $\mathbb{E}[\delta_s]$ in Fig. 9 of the power-efficient algorithm become much larger. The reason can be found in the lack of the absolute total power consumption limited by P_{ctrl}. Under the condition that many gateways are in bad weather conditions or many satellites are at a long distance from gateways, the absolute amount of the total power is insufficient to provide enough power to all the satellites. This inconsistency problem of the proposed algorithm causes a large deviation as P_{ctrl} gets smaller. Fortunately, the deviations of both local sensitivity and the daily average of $\mathbb{E}[\delta_s]$ drastically decrease above the point of diminishing returns. Accordingly, for constructing both stable and consistent networks, P_{ctrl} should be set as 45-55 W, which is above the point of diminishing returns.

VI. CONCLUSION

In this paper, for reliable and low latency control link association, we solved a joint problem of link association and gateway power allocation. The power-efficient SDN control link problem exploits the maximum total power P_{ctrl}, which utilizes the logically centralized property of the control plane. Based on the power control analysis derived from the problem, the power-efficient SDN control link algorithm has been proposed. The key point of the proposed algorithm is to decouple link association and power allocation, given the cross-layer parameter $\frac{\partial L_{gs}}{\partial P_g}\Big|_{P_g=P_0}$. In numerical results, the performance of the algorithm was analyzed in detail and we demonstrated the feasibility of the software-defined LEO satellite network. For the stability of the algorithm, further analysis on local sensitivity and stability was conducted to select the appropriate P_{ctrl}. The management plane should select P_{ctrl} of the proposed algorithm above the point of diminishing marginal returns.

This paper has focused on the control link problem where the controllers transmit the control messages to the satellites, but the problem of the opposite direction, where the satellites transmit the network states to the controllers, should be solved, too. Fortunately, the links established by the proposed algorithm can be exploited from the satellites to the controllers because the algorithm also minimizes the power consumption of the satellites by avoiding severe weather attenuation.

This study can be extended to various future work by presenting and solving problems that have not been discussed previously. We assume that the multi-controller system maintains coherence through east/westbound API. However, a large-scale and coherent control plane can be realized by full analysis on operating cost, synchronization cost, and latency of the controller network, which is left for future work. In addition, future work may include the dynamic placement of VNFs on the satellite network and the comprehensive optimization of the Medium Access Control (MAC) layer, the Network layer and the Transport layer. Further analysis on the coherent control plane and VNF placement in the sky will blueprint the provision of various applications through the software-defined satellite network.

APPENDIX A
PROOF OF CONVEXITY OF THE EXPECTED LATENCY

The second derivative of expected latency L_{gs} with respect to transmit power P_g is given as

$$\frac{\partial^2 L_{gs}}{\partial P_g^2} = \left\{ \frac{2\left(\frac{m\gamma_{th}}{\bar{\gamma}_{gc}}\right)^m}{\Gamma\left(m, \frac{m\gamma_{th}}{\bar{\gamma}_{gc}}\right)} e^{-\frac{m\gamma_{th}}{\bar{\gamma}_{gc}}} + m + 1 - \frac{m\gamma_{th}}{\bar{\gamma}_{gc}} \right\} \times \left(\frac{1}{P_g}\right)^2 \left\{ \frac{1}{\Gamma\left(m, \frac{m\gamma_{th}}{\bar{\gamma}_{gc}}\right)} \right\}^2 \left(\frac{m\gamma_{th}}{\bar{\gamma}_{gc}}\right)^m e^{-\frac{m\gamma_{th}}{\bar{\gamma}_{gc}}}, \tag{23}$$

where the term in the last line (after the multiplication sign $\times$) is positive because the average SNR $\bar{\gamma}_{gc}$ and other parameters are always positive. Accordingly, the expected latency L_{gs} is convex with respect to transmit power P_g if

$$\frac{2\left(\frac{m\gamma_{th}}{\bar{\gamma}_{gc}}\right)^m}{\Gamma\left(m, \frac{m\gamma_{th}}{\bar{\gamma}_{gc}}\right)} e^{-\frac{m\gamma_{th}}{\bar{\gamma}_{gc}}} > \frac{m\gamma_{th}}{\bar{\gamma}_{gc}} - (m+1). \tag{24}$$

Let $x = \gamma_{th}/\bar{\gamma}_{gc}$ be the ratio of SNR threshold to average SNR. Then, the left side term $L(\bar{\gamma}_{gc})$ and the right side $R(\bar{\gamma}_{gc})$ of Eq. (24) can be written as functions of x, respectively:

$$L(x) = \frac{2}{\Gamma(m, mx)} (mx)^m e^{-mx}, \tag{25}$$

$$R(x) = mx - (m+1). \tag{26}$$

We claim that the expected latency is convex with respect to P_g under the condition that m is an integer by proving that $L(x) > R(x)$ for all x and integer $m \geq 1$.

i) If $mx < (m+1)$, it is trivial because $L(x)$ is positive for all x.

ii) If $mx \geq (m+1)$, take the logarithm on both $L(x)$ and $R(x)$ and let $L_1(x)$ and $R_1(x)$ denote the left side and right side,

respectively. Then each is written as

$$L_1(x) = \log \frac{2}{\Gamma(m, mx)} + m \log mx - mx, \quad (27)$$

$$R_1(x) = \log\{mx - (m+1)\}. \quad (28)$$

For integer m, we can rewrite the upper incomplete gamma function $\Gamma(m, mx)$ as $\sum_{i=0}^{m-1} \frac{d^i}{d(mx)^i}(mx)^{m-1}e^{-mx}$ [46]. Then, $L_1(x)$ is written again as

$$L_1(x) = \log 2 - \log \sum_{i=0}^{m-1} \frac{d^i}{d(mx)^i}(mx)^{m-1} + m \log mx. \quad (29)$$

Add $\log \sum_{i=0}^{m-1} \frac{d^i}{d(mx)^i}(mx)^{m-1}$ to both sides and let the left side be $L_2(x)$ and the right side be $R_2(x)$. Then $L_2(x)$ and $R_2(x)$ satisfy the following inequality:

$$\begin{aligned} R_2(x) &= \log\{(mx)^m - 2(mx)^{m-1} - 3(m-1)(mx)^{m-2} \\ &\quad - \cdots - m(m-1)!(mx) - (m+1)(m-1)!\} \\ &\leq log(mx)^m \\ &< log\{2(mx)^m\} = L_2(x). \end{aligned} \quad (30)$$

Accordingly, the expected latency L_{gs} is convex with respect to P_g, where shape factor m is an integer equal to or greater than 1.

REFERENCES

[1] I. F. Akyildiz and A. Kak, "The Internet of Space Things/CubeSats: A ubiquitous cyber-physical system for the connected world," *Comput. Netw.*, vol. 150, pp. 134–149, Feb. 2019.

[2] J. P. Choi, S.-H. Chang, and V. W. S. Chan, "Cross-layer routing and scheduling for onboard processing satellites with phased array antenna," *IEEE Trans. Wireless Commun.*, vol. 16, no. 1, pp. 180–192, Jan. 2017.

[3] J. Liu, Y. Shi, L. Zhao, Y. Cao, W. Sun, and N. Kato, "Joint placement of controllers and gateways in SDN-enabled 5G-satellite integrated network," *IEEE J. Sel. Areas Commun.*, vol. 36, no. 2, pp. 221–232, Feb. 2018.

[4] S. Xu, X.-W. Wang, and M. Huang, "Software-defined next-generation satellite networks: Architecture, challenges, and solutions," *IEEE Access*, vol. 6, pp. 4027–4041, 2018.

[5] M. Kaminskiy, "CubeSat data analysis revision," Goddard Space Flight Center, Greenbelt, MD, USA, Tech. Rep. GSFC/Code 371, Nov. 2015.

[6] D. Kreutz, F. Ramos, P. E. Veríssimo, C. E. Rothenberg, S. Azodolmolky, and S. Uhlig, "Software-defined networking: A comprehensive survey," *Proc. IEEE*, vol. 103, no. 1, pp. 14–76, Jan. 2015.

[7] R. Cohen, L. Lewin-Eytan, J. S. Naor, and D. Raz, "Near optimal placement of virtual network functions," in *Proc. IEEE Conf. Comput. Commun. (INFOCOM)*, Hong Kong, Apr./May 2015, pp. 1346–1354.

[8] Z. Tang, B. Zhao, W. Yu, Z. Feng, and C. Wu, "Software defined satellite networks: Benefits and challenges," in *Proc. IEEE Comput. Commun. IT Appl. Conf.*, Oct. 2014, pp. 127–132.

[9] B. Heller, R. Sherwood, and N. McKeown, "The controller placement problem," in *Proc. 1st Workshop Hot Topics Softw. Defined Netw.*, 2012, pp. 7–12.

[10] Y. Li and M. Chen, "Software-defined network function virtualization: A survey," *IEEE Access*, vol. 3, pp. 2542–2553, 2015.

[11] J. Sherry, S. Hasan, C. Scott, A. Krishnamurthy, S. Ratnasamy, and V. Sekar, "Making middleboxes someone else's problem: Network processing as a cloud service," *ACM SIGCOMM Comput. Commun. Rev.*, vol. 42, no. 4, pp. 13–24, 2012.

[12] "SDN architecture," Open Netw. Found., Palo Alto, CA, USA, Tech. Rep. TR-521, 2016.

[13] H. Kim and N. Feamster, "Improving network management with software defined networking," *IEEE Commun. Mag.*, vol. 51, no. 2, pp. 114–119, Feb. 2013.

[14] T. Rossi, M. De Sanctis, E. Cianca, C. Fragale, M. Ruggieri, and H. Fenech, "Future space-based communications infrastructures based on high throughput satellites and software defined networking," in *Proc. IEEE Int. Symp. Syst. Eng. (ISSE)*, Sep. 2015, pp. 332–337.

[15] J. Zhang, X. Zhang, M. A. Imran, B. Evans, Y. Zhang, and W. Wang, "Energy efficient hybrid satellite terrestrial 5G networks with software defined features," *J. Commun. Netw.*, vol. 19, no. 2, pp. 147–161, Apr. 2017.

[16] I. Chih-Lin, C. Rowell, S. Han, Z. Xu, G. Li, and Z. Pan, "Toward green and soft: A 5G perspective," *IEEE Commun. Mag.*, vol. 52, no. 2, pp. 66–73, Feb. 2014.

[17] P. Gandotra, R. K. Jha, and S. Jain, "Green communication in next generation cellular networks: A survey," *IEEE Access*, vol. 5, pp. 11727–11758, 2017.

[18] M. Werner, C. Delucchi, H. J. Vogel, G. Maral, and J. J. D. Ridder, "ATM-based routing in LEO/MEO satellite networks with intersatellite links," *IEEE J. Sel. Areas Commun.*, vol. 15, no. 1, pp. 69–82, Jan. 1997.

[19] A. Donner, M. Berioli, and M. Werner, "MPLS-based satellite constellation networks," *IEEE J. Sel. Areas Commun.*, vol. 22, no. 3, pp. 438–448, Apr. 2004.

[20] M. Werner, "A dynamic routing concept for ATM-based satellite personal communication networks," *IEEE J. Sel. Areas Commun.*, vol. 15, no. 8, pp. 1636–1648, Oct. 1997.

[21] L. Bertaux, S. Medjiah, P. Berthou, S. Abdellatif, A. Hakiri, P. Gelard, F. Planchou, and M. Bruyere, "Software defined networking and virtualization for broadband satellite networks," *IEEE Commun. Mag.*, vol. 53, no. 3, pp. 54–60, Mar. 2015.

[22] Z. Zhang, B. Zhao, W. Yu, and C. Wu, "Poster: An efficient control framework for supporting the future SDN/NFV-enabled satellite network," in *Proc. 23rd Annu. Int. Conf. Mobile Comput. Netw.*, 2017, pp. 603–605.

[23] X. Yu, W.-M. Lei, L. Song, and W. Zhang, "A routing algorithm based on SDN for on-board switching networks," *J. Inf. Sci. Eng.*, vol. 33, no. 5, pp. 1255–1266, 2017.

[24] Y. Zhu, L. Qian, L. Ding, F. Yang, C. Zhi, and T. Song, "Software defined routing algorithm in LEO satellite networks," in *Proc. Int. Conf. Elect. Eng. Inform. (ICELTICs)*, Oct. 2017, pp. 257–262.

[25] P. Du, S. Nazari, J. Mena, R. Fan, M. Gerla, and R. Gupta, "Multipath TCP in SDN-enabled LEO satellite networks," in *Proc. IEEE MILCOM*, Nov. 2016, pp. 354–359.

[26] M. F. Bari, A. R. Roy, S. R. Chowdhury, Q. Zhang, M. F. Zhani, R. Ahmed, and R. Boutaba, "Dynamic controller provisioning in software defined networks," in *Proc. 9th Int. Conf. Netw. Service Manage. (CNSM)*, Oct. 2013, pp. 18–25.

[27] S. Lange, S. Gebert, T. Zinner, P. Tran-Gia, D. Hock, M. Jarschel, and M. Hoffmann, "Heuristic approaches to the controller placement problem in large scale SDN networks," *IEEE Trans. Netw. Service Manag.*, vol. 12, no. 1, pp. 4–17, Mar. 2015.

[28] A. Papa, T. de Cola, P. Vizarreta, M. He, C. M. Machuca, and W. Kellerer, "Dynamic SDN controller placement in a LEO constellation satellite network," in *Proc. IEEE GLOBECOM*, Dec. 2018, pp. 206–212.

[29] M. Berioli, A. Molinaro, S. Morosi, and S. Scalise, "Aerospace communications for emergency applications," *Proc. IEEE*, vol. 99, no. 11, pp. 1922–1938, Nov. 2011.

[30] J. F. Kurose, *Computer Networking: A Top-Down Approach Featuring the Internet*. New Delhi, India: Pearson Education, 2017.

[31] A. Mehrnia and H. Hashemi, "Mobile satellite propagation channel. Part 1—A comparative evaluation of current models," in *Proc. 21st Century Commun. Village IEEE VTS 50th Veh. Technol. Conf.*, vol. 5, Sep. 1999, pp. 2775–2779.

[32] M. O. Hasna and M. S. Alouini, "Outage probability of multihop transmission over Nakagami fading channels," *IEEE Commun. Lett.*, vol. 7, no. 5, pp. 216–218, May 2003.

[33] M. Abramowitz and I. A. Stegun, *Handbook of Mathematical Functions: With Formulas, Graphs, and Mathematical Tables*, vol. 55. New York, NY, USA: Dover, 1972.

[34] A. Goldsmith, *Wireless communication*. Cambridge, U.K.: Cambridge Univ. Press, 2005.

[35] D. P. Bertsekas and J. N. Tsitsiklis, *Introduction to Probability*, vol. 1. Belmont, MA, USA: Athena Scientific, 2002.

[36] J. Ordonez-Lucena, P. Ameigeiras, D. Lopez, J. J. Ramos-Munoz, J. Lorca, and J. Folgueira, "Network slicing for 5G with SDN/NFV: Concepts, architectures, and challenges," *IEEE Commun. Mag.*, vol. 55, no. 5, pp. 80–87, May 2017.

[37] R. Ferrús, H. Koumaras, O. Sallent, G. Agapiou, T. Rasheed, M.-A. Kourtis, C. Boustie, P. Gélard, and T. Ahmed, "SDN/NFV-enabled satellite communications networks: Opportunities, scenarios and challenges," *Phys. Commun.*, vol. 18, pp. 95–112, Mar. 2016.

[38] S. Boyd and L. Vandenberghe, *Convex Optimization*. Cambridge, U.K.: Cambridge Univ. Press, 2004.

[39] J. P. Choi and V. W. S. Chan, "Resource management for advanced transmission antenna satellites," *IEEE Trans. Wireless Commun.*, vol. 8, no. 3, pp. 1308–1321, Mar. 2009.

[40] Y. Nesterov and A. Nemirovskii, *Interior-Point Polynomial Algorithms in Convex Programming*, vol. 13. Philadelphia, PA, USA: SIAM, 1994.

[41] T. Dreischer, H. Kellermeier, E. Fischer, and B. Wandernoth, "Advanced miniature optical terminal family for inter-satellite links in space communication networks," in *Proc. 4th Eur. Conf. Satell. Commun. (ECSC)*, 1997, pp. 73–78.

[42] M. Kennedy and P. Malet, *Application for Authority to Construct, Launch and Operate the Celestri Multimedia Leo System* document, FCC, 1997.

[43] S. R. Pratt, R. A. Raines, C. E. Fossa, and M. A. Temple, "An operational and performance overview of the IRIDIUM low earth orbit satellite system," *IEEE Commun. Surveys*, vol. 2, no. 2, pp. 2–10, 2nd Quart., 1999.

[44] *Globalstar Satellite Phone*. Accessed: Aug. 7, 2019. [Online]. Available: https://www.pivotel.co.nz/pivotel_globalstar_international_coverage

[45] "Enhanced network survivability performance," ANSI, New York, NY, USA, Tech. Rep. t1.tr.68-2001, 2001.

[46] U. Blahak, "Efficient approximation of the incomplete gamma function for use in cloud model applications," *Geosci. Model Develop.*, vol. 3, no. 2, pp. 329–336, 2010.

WONCHEOL CHO received the B.S. degree from the Daegu Gyeongbuk Institute of Science and Technology (DGIST), Daegu, South Korea, in 2018, where he is currently pursuing the M.S. degree with the Department of Information and Communication Engineering. His research interests include the cross-layer optimization of satellite networks and 5G service in wireless networks.

JIHWAN P. CHOI (S'01–M'06–SM'17) received the B.S. degree in electrical engineering from Seoul National University, Seoul, South Korea, and the S.M. and Ph.D. degrees in electrical engineering and computer science from the Massachusetts Institute of Technology (MIT), Cambridge, MA, USA. He was a Principal System Engineer with the Wireless Research and Development Group, Marvell Semiconductor Inc., Santa Clara, CA, USA, for mobile system design and standardization of 4G wireless networks. He is currently an Associate Professor with the Department of Information and Communication Engineering, Daegu Gyeongbuk Institute of Science and Technology (DGIST), Daegu, South Korea. He has served as an ICT Research and Development Planner with the Institute for Information and Communications Promotion (IITP), South Korea, from 2016 to 2017, where he designed government Research and Development projects and strategies on satellite communications. He is currently an Associate Editor of the IEEE TRANSACTIONS ON AEROSPACE AND ELECTRONIC SYSTEMS and IEEE ACCESS. His research interests include cross-layer design of space and wireless networks, and the applications of machine learning.